Atom lithography with near-resonant standing waves

R. Arun, Offir Cohen, and I. Sh. Averbukh
Department of Chemical Physics, The Weizmann Institute of Science, Rehovot 76100, Israel
(Received 1 April 2010; published 9 June 2010)

We study the optimal focusing of two-level atoms with a near-resonant standing wave light, using both classical and quantum treatments of the problem in the thin- and thick-lens regimes. It is found that the near-resonant standing wave focuses the atoms with a reduced background in comparison with far-detuned light fields. For some parameters, the quantum atomic distribution shows even better localization than the classical one. Spontaneous emission effects are included via the technique of quantum Monte Carlo wave function simulations. We investigate the extent to which nonadiabatic and spontaneous emission effects limit the achievable minimal size of the deposited structures.

DOI: 10.1103/PhysRevA.81.063809 PACS number(s): 42.50.Wk, 37.10.Vz, 03.75.Be, 42.82.Cr

I. INTRODUCTION

The ability to control the motion of atoms using laser fields has led to the realization of optical elements such as mirrors, lenses, beam splitters, and so on, for atomic beams. One of the interesting applications is the laser focusing of atoms, which is useful to the technology of atom lithography. The principle of atom lithography is based on using a standing wave (SW) of light as a mask on atoms to concentrate the atomic flux periodically and create desired patterns at the nanometer scale (for recent reviews see Refs. [1,2]). Since the first experimental demonstration of submicron atomic structures [3], the subject has seen a considerable growth both theoretically [4–8] and experimentally [9–15]. In the direct deposition setup, periodic atomic lines of sodium [3,9], chromium [10,11], aluminum [12], ytterbium [13], and iron [14] atoms have been successfully fabricated. The technique has also been applied to two-dimensional pattern formation [15].

Theoretical studies of atom lithography commonly employ a particle optics approach to laser focusing of atoms [4,5,16]. The focal properties of the light SWs have been examined in terms of time-dependent classical trajectories of atoms in the light induced potential. It has been shown that the atomic image at the focal plane exhibits a broadening due to severe aberrations caused by anharmonicity of the sinusoidal dipole potential [4,5]. As a result, all current lithography schemes suffer from a considerable background in the deposited structures. The aberration problem may be effectively resolved by using optimized multilayer light masks, as was shown in Ref. [16]. Quantum mechanical analysis of the focusing of atomic beams has been performed as well. Cohen *et al.* studied quantum mechanically the thin-lens regime of atom focusing with both far detuned and exactly resonant standing light waves [6]. Atomic nanostructures produced by exactly resonant SW were experimentally demonstrated in Ref. [17]. In the thick-lens regime, the process of atomic focusing is generally achieved with a blue-detuned SW light whose detuning (Δ) is of the order of the Rabi frequency (Ω_0) characterizing the strength of the atom-light interaction [4,5]. In this case, the influence of spontaneous emission on the focusing of atoms has been shown to be negligible by the quantum treatment [8].

Optimizing the feature resolution achievable in atom lithography has been studied both in the far off-resonance [16] and on-resonance [18] regimes, by means of optimal light mask configuration, requiring several light sources. In this article, we investigate in detail the focusing properties of a single SW light mask and explore the ways for reduction in spherical aberrations. Specifically, we concentrate on the near-resonant case ($|\Delta|/\Omega_0 \lesssim 1$), considering both blue- and red-detuned light, and give a comprehensive theoretical analysis for both the classical and quantum treatments of the problem. The parameters for the best focusing of atoms are found as functions of the detuning ($|\Delta|$) using the optimization procedure developed in Ref. [16]. To include momentum diffusion and spontaneous emission effects on atoms, we perform Monte Carlo wave function simulations. High-resolution deposition of chromium atoms is considered as an example, though the general conclusions drawn should apply well to other atoms.

The article is arranged as follows. In Sec. II, the basic framework of the problem is defined and the focusing of atoms is studied classically under the influence of adiabatic light potentials. In this section, we examine the optimal focusing scheme of Ref. [16] when applied to the atomic-beam traversing a near-resonant SW light. In Sec. III, the problem is treated in the quantum domain to account for nonadiabatic and diffraction effects on atom focusing. The effects of spontaneous emission of atoms are considered in Sec. IV. Finally, in Sec. V, we summarize our main results.

II. FOCUSING OF ATOMS BY ADIABATIC LIGHT POTENTIALS: CLASSICAL TREATMENT

We begin our discussion with a model based on the interaction of a beam of two-level atoms with a near-resonant SW light. We take the direction of propagation of the atomic beam through the light along the z direction. The SW (assumed to be formed along the x direction) has a frequency of ω_l and $\Delta = \omega_l - \omega_0$ defines the detuning of the light frequency from the atomic transition frequency ω_0. The atom-light interaction is characterized by the Rabi frequency

$$\Omega(x,z) = \Omega_0 \exp\left(-z^2/\sigma_z^2\right) \cos(kx). \tag{1}$$

Here, the term $\exp(-z^2/\sigma_z^2)$ accounts for the spatial variation (a Gaussian beam profile with diameter σ_z) of the light intensity

along the z direction. The $\cos(kx)$ term comes from the sinusoidal $[I(x) \propto \cos^2(kx)]$ variation of the SW intensity along the x direction. The quantity Ω_0 represents the peak Rabi frequency of the atom-light interaction and $\lambda = 2\pi/k$ is the wavelength of the laser beams forming the SW. The velocity v_z of the atoms along the beam axis is sufficiently large, so the atom's position along the z direction can be replaced by the time dependence $z = v_z t$. Defining $\sigma_t = \sigma_z/v_z$, the time-dependent Rabi frequency is thus given by

$$\Omega(x,t) = \Omega_0 \exp\left(-t^2/\sigma_t^2\right) \cos(kx). \tag{2}$$

The behavior of atoms in the near-resonant light field can be best understood in the dressed state picture of the atom-light interaction [19]. The dressed states, which are the eigenstates of the interaction Hamiltonian, depend on time through the time-dependent Rabi coupling Eq. (2). If the Hamiltonian temporal variation is smooth, the atom prepared initially in one of the eigenstates of the Hamiltonian will follow the time-dependent eigenstate. The corresponding adiabatic condition is [20]

$$|\Delta| \gg \sqrt{\frac{\Omega_0}{\sigma_t}}. \tag{3}$$

We assume that the atoms in the beam are initially in their ground state and that the adiabatic condition Eq. (3) is satisfied. In this case, the atoms can be described as pointlike particles moving in the potential

$$U(x,t) = \mathrm{sgn}(\Delta)\frac{\hbar}{2}\sqrt{\Delta^2 + \Omega^2(x,t)}. \tag{4}$$

Here $\mathrm{sgn}(\Delta) = +1(-1)$ for $\Delta > 0$ $(\Delta < 0)$. Note that this adiabatic potential should be contrasted with the light shift felt by the bare atomic states in the far-detuned limit [6]. The adiabatic potentials and the focusing of atoms are shown schematically in Fig. 1.

Many aspects of atom focusing by the standing light waves can be explained in the semiclassical picture of the atom's interaction with the light-induced potential [4,5,16]. Therefore, we start considering the problem in the classical framework. We neglect spontaneous emission from the atoms by assuming that the atom's interaction time with the light is much shorter compared to the lifetime of the excited atomic level. The classical trajectories of atoms in the adiabatic light potential Eq. (4) obey Newton's equation of motion

$$\frac{d^2x}{dt^2} + \frac{1}{m}\frac{\partial U(x,t)}{\partial x} = 0, \tag{5}$$

where m is the atomic mass. The force induced by the SW focuses (localizes) the atoms near the intensity minima (maxima) for $\Delta > 0$ $(\Delta < 0)$. As a measure of the atomic localization, we use the localization factor [16]

$$\begin{aligned} L(t) &= 1 + \mathrm{sgn}(\Delta)\langle \cos\left[2kx(t,x_0)\right]\rangle \\ &\equiv \frac{2}{\lambda}\int_{-\lambda/4}^{\lambda/4} dx_0\{1 + \mathrm{sgn}(\Delta)\cos[2kx(t,x_0)]\}, \end{aligned} \tag{6}$$

where $x(t,x_0)$ is the solution of the differential Eq. (5) satisfying the initial condition $x \to x_0$ at $t \to -\infty$. The average in Eq. (6) is taken over the random initial positions of the atoms, and the localization factor is measured as

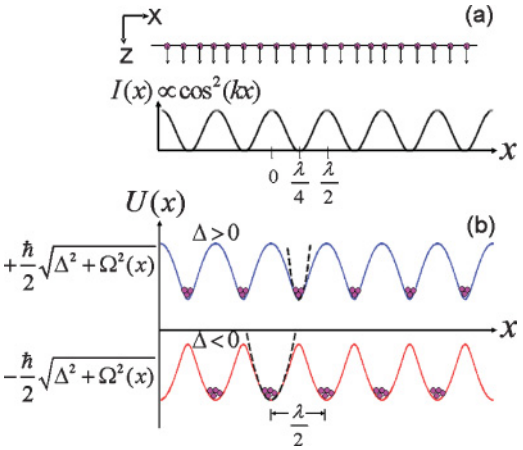

FIG. 1. (Color online) Schematic representation of laser focusing of atoms by a SW light. (a) A collimated atomic beam impinges on the near-resonant SW light whose intensity varies sinusoidally along the x direction. (b) The interaction with the light induces the adiabatic potential [either plus or minus in Eq. (4)] for the external motion of atoms depending upon the sign of the detuning. For a positive (blue) detuning, the atoms localize near the minima of the light intensity, while for a negative (red) detuning they get localized near the light intensity maxima. The dashed curves represent the quadratic approximation to the adiabatic potentials near their minima.

a function of time t counted from the moment $(t = 0)$ of passing the Gaussian center of the SW. The localization factor equals zero for an ideally localized atomic ensemble and is proportional to the mean-square variation of the x coordinate (modulo standing-wave period) in the case of a well-localized distribution $(L \ll 1)$.

The localization factor defined in Eq. (6) measures a nonlinear spatial focusing of atoms beyond the linear paraxial approximation. According to the optimal focusing theory [16], minimal background in the atom deposition is not achieved at the focal plane but occurs for the parameters providing global minimum of the localization factor. The optimal parameters can be obtained either in the thin- or thick-lens limit of atom focusing. First, we consider the thin-lens focusing [3] of atoms by the adiabatic potential Eq. (4), which is valid in the Raman-Nath approximation to the atom-light interaction. In this case, the atomic displacement along the SW direction is negligible within the light and the focal point is well outside the region of the light fields [5]. Within thin-lens approximation, the SW introduces a spatially dependent sudden kick to the atoms along the transverse (x axis) direction. The change in velocity can be calculated from Eq. (5) as

$$\begin{aligned} \delta v_x = \mathrm{sgn}(\Delta)&\frac{\hbar k \Omega_0^2}{4m} \\ &\times \int dt \frac{\exp\left(-2t^2/\sigma_t^2\right)\sin[2kx(t)]}{\sqrt{\Delta^2 + \Omega_0^2 \exp\left(-2t^2/\sigma_t^2\right)\cos^2[kx(t)]}}. \end{aligned} \tag{7}$$

In the Raman-Nath approximation, the position $x(t)$ of the atom in Eq. (7) during interaction with the light can be approximated to be its initial position x_0. After passing through the light region, the atom (that is assumed to have zero initial

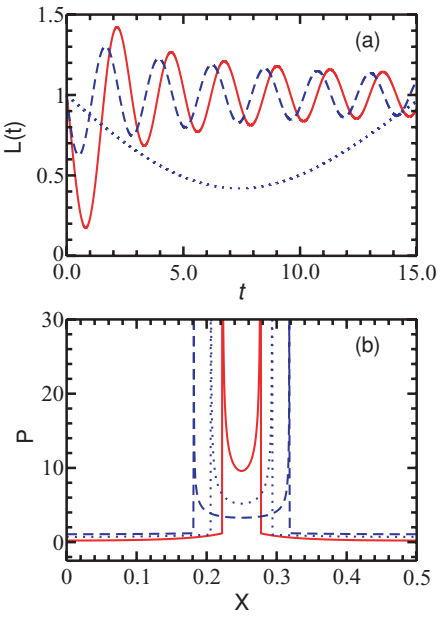

FIG. 2. (Color online) (a) Localization factor of the atomic distribution as a function of the dimensionless time t for $\sigma_t = 0.07$ and $\Delta/\Omega_0 = -0.125$ (solid curve), $\Delta/\Omega_0 = 0.125$ (dashed curve), $\Delta/\Omega_0 = 5$ (dotted curve). The global minimum values of $L(t)$ are 0.17 (solid curve), 0.63 (dashed curve), and 0.42 (dotted curve). (b) Probability density (P) of the atomic distribution at the time $t = t_m$ of the best atomic localization. The parameters are same as those of (a) with $t_m = 0.82$ (solid curve), $t_m = 0.52$ (dashed curve), and $t_m = 7.38$ (dotted curve). For the sake of comparison, the solid curve has been displaced by 0.25 units along the X axis. The times t_m correspond to the global minima of the localization factor in (a).

velocity along the x axis) moves as a free particle with a time-dependent transverse position

$$x(t,x_0) = x_0 + \delta v_x t. \tag{8}$$

Using Eqs. (6) and (8), we calculate the localization factor as a function of dimensionless time (see below) for both blue ($\Delta > 0$) and red ($\Delta < 0$) detuning conditions. The results are shown in Fig. 2 with plots of the atomic distribution [21] at the time of minimal localization factor. These results are also compared with the best atomic localization that can be achieved with the usual far-detuned ($\Delta/\Omega_0 \gg 1$) SW light. We use dimensionless variables in which position is measured in units of the optical wavelength (λ), frequency in units of the recoil frequency ($\omega_{\rm rec} \equiv \hbar k^2/2m$), and time in units of $1/[\omega_{\rm rec}\Omega_0\sigma_t]$. It is seen from the graph that the near-resonant light with red detuning from the atomic transition focuses the atoms better compared with the far-detuned light, i.e., the former suffers less spherical aberrations. The atomic localization improves as the magnitude of the red detuning decreases. This is shown in Fig. 3(a), where we plot the best localization factor as a function of the detuning parameter (Δ/Ω_0). Note that the localization factor saturates to the well-known value of $L \approx 0.42$ in the far-detuned ($|\Delta|/\Omega_0 \gg 1$) case [16]. It tends to the asymptotic value of $L \approx 0.1$ for $\Delta \to 0^-$. We note, however, that nonadiabatic quantum effects should be taken into account when the adiabatic condition, Eq. (3) fails (see the next section).

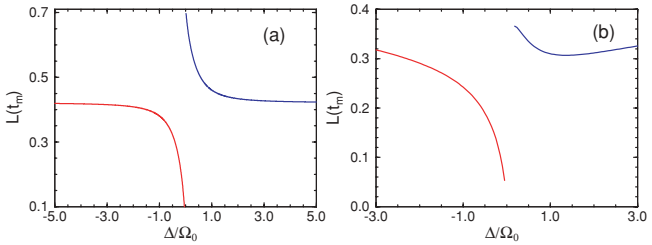

FIG. 3. (Color online) Classical treatment. Minimal localization factor of the atomic distribution as a function of the detuning Δ/Ω_0 for (a) thin lens, $\sigma_t = 0.07$, and (b) thick lens, $\sigma_t = 4$.

In the opposite limit of the thick lens, the atoms are focused within the region of the light fields [5]. The atom focusing in this limit is very similar to the operation of the graded index lens in traditional optics. Neglecting the time dependence in the Rabi frequency, we find the focal length in the paraxial approximation as

$$f = \frac{v_z\pi}{2\Omega_0}\sqrt{\frac{\Delta}{\omega_{\rm rec}}} \quad [\Delta > 0, \text{ thick lens}],$$
$$f = \frac{v_z\pi}{2\Omega_0}\sqrt{\frac{\sqrt{\Delta^2+\Omega_0^2}}{\omega_{\rm rec}}} \quad [\Delta < 0, \text{ thick lens}]. \tag{9}$$

From the above expressions, it is seen that the focal length is greater for red detuning. To go beyond the paraxial approximation, the solution $x(t)$ of the atomic motion needs to be obtained directly by the numerical integration of Eq. (5). Using Eqs. (5) and (6), we obtain the localization factor of the atomic distribution as shown in Figs. 3(b) and 4.

Comparing the graphs in Figs. 2 and 4, we see a qualitative similarity between the thin- and thick-lens focusing of atoms. In particular, focusing atoms by the red-detuned light gives rise to a much reduced background of deposited atoms in comparison to the case of atom focusing by the blue-detuned light. In the paraxial approximation, this can be explained by

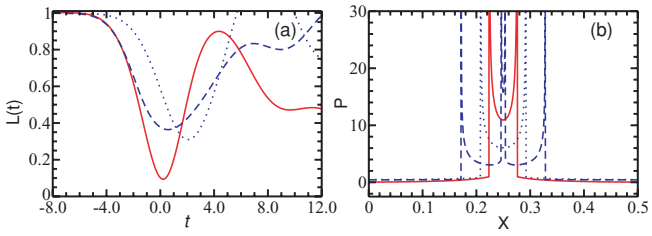

FIG. 4. (Color online) (a) Localization factor of the atomic distribution as a function of the dimensionless time t for $\sigma_t = 4$ and $\Delta/\Omega_0 = -0.125$ (solid curve), $\Delta/\Omega_0 = 0.125$ (dashed curve), $\Delta/\Omega_0 = 1$ (dotted curve). The global minimum values of $L(t)$ are 0.1 (solid curve), 0.36 (dashed curve), and 0.31 (dotted curve). (b) Probability density (P) of the atomic distribution at the time $t = t_m$ of the best atomic localization. The parameters are same as those of (a) with $t_m = 0.2$ (solid curve), $t_m = 0.58$ (dashed curve), and $t_m = 2$ (dotted curve). For the sake of comparison, the solid curve has been displaced by 0.25 units along the x axis. The times t_m correspond to the global minima of the localization factor in (a).

expanding the adiabatic potentials Eq. (4) up to the quadratic terms (parabolic fitting) near the potential minima [22]. As shown in Fig. 1, the spatial range, in which the quadratic approximation is valid, is wider for the case of negative detuning (Δ), which results in the reduced aberrations. We note again that the above analysis is valid only in the range of parameters for which the adiabatic condition Eq. (3) is satisfied. For smaller detunings ($|\Delta|/\Omega_0 \ll 1$), nonadiabatic and quantum effects may dominate. This is examined in the next section.

III. OPTIMAL ATOMIC FOCUSING: EFFECTS OF THE WAVE NATURE OF ATOMS

In the classical treatment of atom focusing discussed so far, the internal structure of the atom was completely ignored and the atomic motion in a single adiabatic potential was studied. This procedure is valid even if the atomic motion is treated quantum mechanically, provided the adiabatic condition (3) is satisfied. In the quantum treatment, the atomic center-of-mass wave function $\psi(x,t)$ evolves in time according to Schrödinger equation with the potential $U(x,t)$ given by Eq. (4):

$$i\hbar\frac{\partial}{\partial t}\psi(x,t)=\left[\frac{p_x^2}{2m}+U(x,t)\right]\psi(x,t), \tag{10}$$

where p_x denotes the center-of-mass momentum operator of the atom along the SW (x axis) direction.

Equation (10) is useful to study the quantum effects in the far off-resonant atom focusing. The situation becomes more complicated if the light detuning is relatively small ($|\Delta| \ll \Omega_0$). In this case, nonadiabatic effects arise from transitions between the dressed atomic states. Therefore, in order to cover a wide range of detunings while taking into account the nonadiabatic transitions, we consider the evolution of the atomic wave function directly in the bare-states basis, first neglecting spontaneous emission from the atoms. The Hamiltonian for a two-level atom with excited ($|e\rangle$) and ground ($|g\rangle$) states interacting with the SW light is given by

$$H(t)=\frac{p_x^2}{2m}-\frac{\hbar\Delta}{2}(|e\rangle\langle e|-|g\rangle\langle g|)+\frac{\hbar\Omega(x,t)}{2}(|e\rangle\langle g|+|g\rangle\langle e|), \tag{11}$$

where $\Omega(x,t)$ is given by Eq. (2).

The wave function of the two-level atom may be expressed as

$$\Psi(x,t)=\begin{bmatrix}\psi_e(x,t)\\ \psi_g(x,t)\end{bmatrix}. \tag{12}$$

Here $\psi_{e,g}(x,t)$ correspond to the center-of-mass wave functions of the atom in its excited and ground states. We consider a spatially uniform beam of ground state atoms having initially zero momentum along the SW direction. The initial wave function of the atom normalized over the region of the SW period [21] is then given by $\psi_g(x,t_0)=\sqrt{2/\lambda}$, where the initial time $t_0 \to -\infty$. Since the atomic distribution is expected to be periodic (in space) after interaction with the light field, the wave functions at time t can be Fourier expanded as

$$\psi_e(x,t)=\sum_{n=-\infty}^{n=\infty}C_n^e(t)e^{i(2n+1)kx},\qquad \psi_g(x,t)=\sum_{n=-\infty}^{n=\infty}C_n^g(t)e^{i2nkx}. \tag{13}$$

The Fourier coefficients $C_n^e(t)$ and $C_n^g(t)$, defined above, represent the probability amplitudes for finding the atom in the excited and ground states with momentum $(2n+1)\hbar k$ and $2n\hbar k$, respectively. Using Eqs. (11)–(13), the Schrödinger equation $i\hbar\partial\Psi/\partial t = H\Psi$ then leads to the coupled equations for the Fourier amplitudes:

$$\begin{aligned} i\frac{d}{dt}C_n^e(t)&=\left\{(2n+1)^2\omega_{\rm rec}-\frac{\Delta}{2}\right\}C_n^e(t)+\frac{\Omega(t)}{4}\left[C_n^g(t)+C_{n+1}^g(t)\right],\\ i\frac{d}{dt}C_n^g(t)&=\left\{4n^2\omega_{\rm rec}+\frac{\Delta}{2}\right\}C_n^g(t)+\frac{\Omega(t)}{4}\left[C_n^e(t)+C_{n-1}^e(t)\right], \end{aligned} \tag{14}$$

with $\Omega(t)=\Omega_0\exp(-t^2/\sigma_t^2)$.

We now proceed to the calculation of the quantum localization factor defined as

$$\begin{aligned} L(t)&=1+\mathrm{sgn}(\Delta)\langle\cos(2kx)\rangle\\ &\equiv 1+\mathrm{sgn}(\Delta)\int_{-\lambda/4}^{\lambda/4}dx|\Psi(x,t)|^2\cos(2kx). \end{aligned} \tag{15}$$

The atomic density $|\Psi(x,t)|^2=|\psi_e(x,t)|^2+|\psi_g(x,t)|^2$ is found using Eq. (13). For the initial beam of ground-state atoms $C_0^g(-\infty)=\sqrt{2/\lambda}$. The localization factor can be obtained by solving numerically Eq. (14):

$$L(t)=1+\mathrm{sgn}(\Delta)\frac{\lambda}{2}\mathrm{Re}\sum_{n=-\infty}^{n=\infty}\left[C_n^e(t)C_{n+1}^e(t)^*+C_n^g(t)C_{n+1}^g(t)^*\right]. \tag{16}$$

As discussed in the previous section, the best spatial localization of atoms occurs at the time $t=t_m$ of the global minimum of the localization factor. To minimize the localization factor Eq. (16), we first rescale the time variable t in terms of the recoil time $t_{\rm rec}\equiv 1/\omega_{\rm rec}$. In the classical analysis of atom focusing, we used a time scale that depends on the strength (Ω_0) of the atom-light interaction. However, a quantized space-periodic motion of ground state atoms in free space [23] repeats itself (in time) after each revival period of $t_R=\pi t_{\rm rec}/2$. It is therefore convenient to use the recoil time $t_{\rm rec}$ for scaling the variables t and σ_t.

In Figs. 5 and 6, we display the localization factor and the atomic spatial density for the thin-lens focusing of atoms. Comparing the quantum mechanical localization factor with its classical counterpart (see Figs. 2 and 5), we see that they have the same structure for short times and the same minimal values for both blue- and red-detuning situations. However, the localization factor differs considerably in the long time

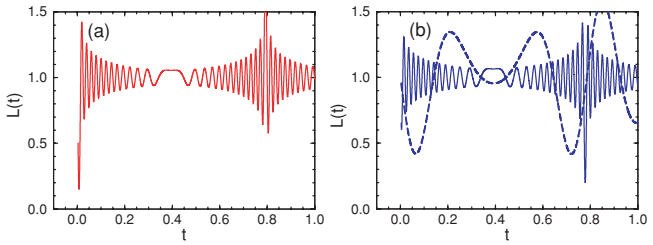

FIG. 5. (Color online) Localization factor of the atomic distribution as a function of the dimensionless time t for the parameters $\sigma_t = 0.0006$, $\Omega_0 = 1.92 \times 10^5$, and (a) $\Delta/\Omega_0 = -0.125$, (b) $\Delta/\Omega_0 = 0.125$ (solid curve), $\Delta/\Omega_0 = 5$ (long-dashed curve). The global minimum values of $L(t)$ are (a) 0.15, and (b) 0.2 (solid curve), 0.42 (long-dashed curve).

evolution of the atomic distribution. It reaches a new minimum value of $L = 0.2$ at about half of the revival period for the blue detuned ($\Delta/\Omega_0 = 0.125$) light [24]. Due to these distinct quantum features in the atom localization, the quantum atomic distribution becomes narrower than the classical distribution [compare Figs. 2(b) and 6] in the atom focusing by the blue-detuned light. Next, we show the best quantum localization of atoms that can be achieved by varying the detuning [Fig. 7(a)]. Again, comparing it with the classical result [see Fig. 3(a)], it is seen that they are identical for the red-detuning ($\Delta < 0$) case. New quantum features exist only in the focusing of atoms by the blue-detuned light ($\Delta > 0$). For the thick-lens focusing of atoms, the results are shown in Figs. 7(b) and 8. In this case, the quantum and classical results are quite similar in the adiabatic regime of atom focusing and there are no distinct quantum features in the localization of atoms. The wave effects in propagation have a limited manifestation in this case due to the relatively short focal length.

When the light frequency is tuned very close to the atomic resonance ($|\Delta| \ll \Omega_0$), the adiabatic potentials, Eq. (4), experience sharp spatial variations along the x coordinate in the regions of avoided crossings near the nodes of the SW. As a result, nonadiabatic effects degrade greatly the focusing of atoms. In this case, the atoms do not follow single adiabatic

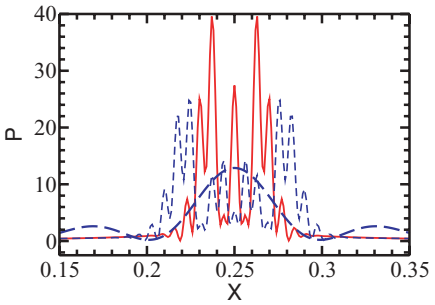

FIG. 6. (Color online) Probability density ($P = |\Psi(x,t)|^2$) of the atomic distribution at the time $t = t_m$ of the best atomic localization. The parameters are $\sigma_t = 0.0006$, $\Omega_0 = 1.92 \times 10^5$, and $\Delta/\Omega_0 = -0.125$, $t_m = 7 \times 10^{-3}$ (solid curve), $\Delta/\Omega_0 = 0.125$, $t_m = 0.778$ (dashed curve), $\Delta/\Omega_0 = 5$, $t_m = 0.72$ (long-dashed curve). For the sake of comparison, the solid curve has been displaced by 0.25 units along the x axis. The times t_m correspond to the global minima of the localization factor in Fig. 5.

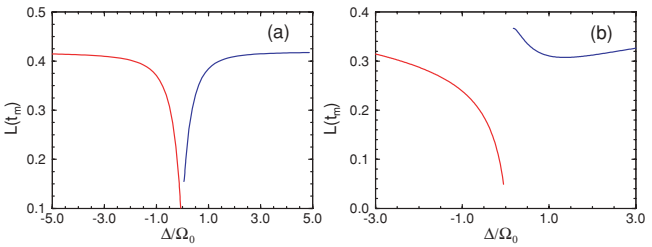

FIG. 7. (Color online) Quantum treatment. Minimal localization factor of the atomic distribution as a function of the detuning Δ/Ω_0 for (a) thin lens, $\sigma_t = 0.0006$, and (b) thick lens, $\sigma_t = 0.01$.

potential [either plus or minus in Eq. (4)] during the interaction with the SW but rather make random transitions between them in the regions of quasicrossing. As a result, they tend to focus near both the minima and maxima of the light intensity with no well-defined localization region, as shown in Fig. 9 for the thick-lens focusing. The localization factor defined in Eq. (15) is not appropriate to characterize the atomic distribution for this case. It is to be noted that the result of splitting of atomic wave packets (similar to Fig. 9) by nonadiabatic effects is a common feature in the thin-lens regime as well. In fact, we have verified this numerically and found that our numerical results are consistent with the analytical study of atom focusing using resonant SW's considered in Ref. [6].

IV. MONTE CARLO SIMULATIONS

We have so far simplified the classical and quantum treatments of the problem by assuming that the atoms do not change their internal states by spontaneous emission during the interaction with the light. This is strictly valid for far-detuned light fields when an adiabatic elimination of the excited atomic level may be performed [6]. However, for atoms interacting with the near-resonant SW, the restriction to include

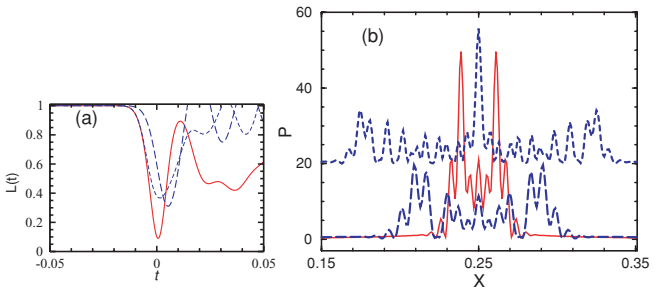

FIG. 8. (Color online) (a) Localization factor of the atomic distribution as a function of the dimensionless time t for the parameters $\sigma_t = 0.01$, $\Omega_0 = 4 \times 10^4$, and $\Delta/\Omega_0 = -0.125$ (solid curve), $\Delta/\Omega_0 = 0.125$ (dashed curve), $\Delta/\Omega_0 = 1$ (long-dashed curve). The global minimum values of $L(t)$ are 0.1 (solid curve), 0.37 (dashed curve), and 0.31 (long-dashed curve). (b) Probability density ($P = |\Psi(x,t)|^2$) of the atomic distribution at the time $t = t_m$ of the best atomic localization. The parameters are same as those of (a) with $t_m = 0$ (solid curve), $t_m = 1.5 \times 10^{-3}$ (dashed curve), and $t_m = 5.3 \times 10^{-3}$ (long-dashed curve). For the sake of comparison, we have displaced the solid curve by 0.25 units along the x axis and the dashed curve by 20 units along the P axis. The times t_m correspond to the global minima of the localization factor in (a).

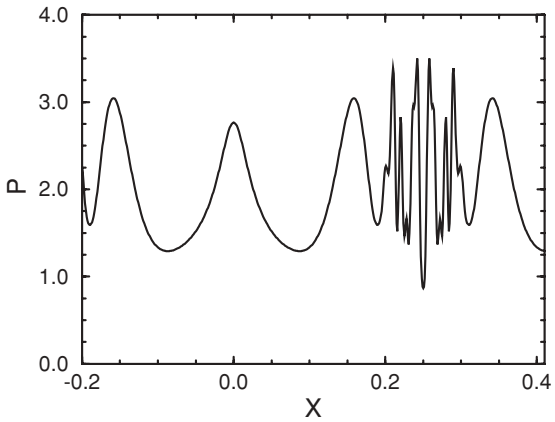

FIG. 9. Probability density ($P = |\Psi(x,t)|^2$) of the atomic distribution for the parameters $\sigma_t = 0.01$, $\Omega_0 = 2 \times 10^4$, $t = 0$, and $\Delta/\Omega_0 = 10^{-2}$.

spontaneous emissions may be relaxed only if $\Gamma\sigma_t \ll 1$, where Γ is the decay rate of the excited atomic level. In the specific case of the chromium atom ($\Gamma = 238$ in units of the recoil frequency $\omega_{\rm rec}$) deposition which we consider, the quantity $\Gamma\sigma_t$ becomes of the order of 0.1 and 2 in the thin ($\sigma_t = 0.0006$) and thick ($\sigma_t = 0.01$) lens regimes, respectively. Therefore, it is necessary to study the extent to which spontaneous emission degrades the focusing performance of the adiabatic light potentials.

The effects of spontaneous emission on the focusing of atoms are twofold. First, it may modify the trajectories of atoms by imparting momentum kicks in random directions. Second, the dressed internal state of the atom changes due to spontaneous emissions, resulting in random jumps between the plus and minus adiabatic potentials [see Eq. (4)] that the atom experiences. To model all these features, we employ the quantum Monte Carlo wave function (MCWF) simulations [25,26] for the description of atoms emitting spontaneous photons and moving in a SW light field. In this approach, the atomic density P is calculated by forming N realizations of quantum trajectories $\psi^s_{e,g}(x,t)$ and then averaging over them:

$$P \equiv |\Psi(x,t)|^2 = \frac{1}{N}\sum_{s=1}^{N}\left[\left|\psi^s_e(x,t)\right|^2 + \left|\psi^s_g(x,t)\right|^2\right]. \quad (17)$$

Each quantum trajectory $\psi^s_{e,g}(x,t)$ consists of a set of deterministic Hamiltonian evolution periods interrupted by quantum collapses. The evolution is governed by a non-Hermitian Hamiltonian $H_{\rm eff} = H(t) - i\hbar(\Gamma/2)|e\rangle\langle e|$, where the term $H(t)$ describes the coherent dynamics of the atom-light interaction as given in Eq. (11) and the imaginary term (containing Γ) accounts for the spontaneous decay of the excited atomic level. The collapse of the atomic wave function is given by the action of the operator

$$C_{k'} = [\Gamma N(k')]^{1/2}\exp(-ik'x)|g\rangle\langle e|, \quad (18)$$

where

$$N(k') = (3/8k)\left[1 + \left(\frac{k'}{k}\right)^2\right] \quad (19)$$

is the normalized probability density for the distribution of the spontaneously emitted photons with the momentum component $\hbar k'$ along the SW direction (x axis).

When there is no spontaneous emission event, the internal states of the atom are coupled only by stimulated processes. The atomic wave function at time t is given by a Fourier series [cf. Eq. (13)]

$$\begin{aligned}\psi_e(x,t) &= \sum_{n=-\infty}^{n=\infty} C^e_n(t,t_i)e^{i[p_0+(2n+1)\hbar k]x/\hbar},\\ \psi_g(x,t) &= \sum_{n=-\infty}^{n=\infty} C^g_n(t,t_i)e^{i[p_0+2n\hbar k]x/\hbar},\end{aligned} \quad (20)$$

where p_0 is the momentum of the atom along the SW direction at the initial time t_i. The Fourier coefficients defined above depend on the initial time t_i and evolve with time t (until a spontaneous emission takes place) as governed by the non-Hermitian Hamiltonian $H_{\rm eff}$:

$$\begin{aligned} i\frac{d}{dt}C^e_n(t) &= \left\{\frac{[p_o+(2n+1)\hbar k]^2}{2m\hbar} - \frac{\Delta}{2} - \frac{i\Gamma}{2}\right\}C^e_n(t)\\ &\quad + \frac{\Omega(t)}{4}\left[C^g_n(t) + C^g_{n+1}(t)\right],\\ i\frac{d}{dt}C^g_n(t) &= \left\{\frac{[p_o+2n\hbar k]^2}{2m\hbar} + \frac{\Delta}{2}\right\}C^g_n(t)\\ &\quad + \frac{\Omega(t)}{4}\left[C^e_n(t) + C^e_{n-1}(t)\right].\end{aligned} \quad (21)$$

If a spontaneous emission from the atom takes place at the time t, the momentum $\hbar k'$ of the spontaneously emitted photon is chosen randomly according to the probability law $N(k')$ [Eq. (19)] and the collapse of the atomic wave function to the ground state is carried out with the operator Eq. (18) as follows

$$\begin{aligned} C^g_n(t) &= C^e_n(t)\Big/\sqrt{(\lambda/2)\sum_n \left|C^e_n(t)\right|^2},\\ C^e_n(t) &= 0,\\ p_0 &\to p_0 + \hbar k - \hbar k'.\end{aligned} \quad (22)$$

In the MCWF simulations [26], the random moment t at which the spontaneous emission takes place is chosen when the decaying total norm of the atomic wave function reaches the value of $1-\varepsilon$, where $\varepsilon \in [0,\ldots 1]$ is a random number uniformly distributed between 0 and 1. The moment of emission is determined by solving the equation

$$1 - (\lambda/2)\sum_{n=-\infty}^{n=\infty}\left[\left|C^e_n(t,t_i)\right|^2 + \left|C^g_n(t,t_i)\right|^2\right] = \varepsilon. \quad (23)$$

We take the initial time t_i to be $-5\sigma_t$ (instead of $-\infty$) at which the Rabi frequency $\Omega(x,t)$ [Eq. (2)] drops significantly compared to its peak value. We assume, as before, the initial condition in the form of an atomic plane wave in the ground state with zero transverse momentum ($p_0 = 0$). The norm $|\Psi(t)|^2 = (\lambda/2)\sum_n[|C^e_n(t,t_i)|^2 + |C^g_n(t,t_i)|^2]$ of the wave function is then obtained by solving Eq. (21) until the time $t = t_{MC}$ at which Eq. (23) is fulfilled. At this moment, we collapse the atomic wave function to the ground state and

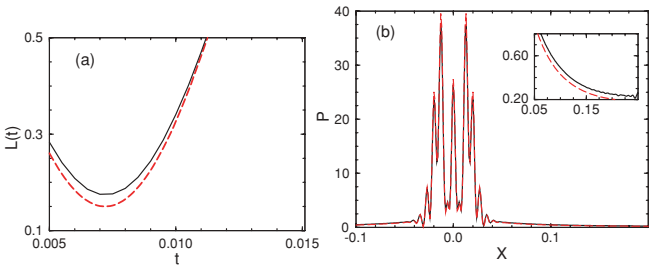

FIG. 10. (Color online) (a) Localization factor of the atomic distribution as a function of the dimensionless time t around its global minimum for the parameters $\sigma_t = 0.0006$, $\Omega_0 = 1.92 \times 10^5$, $\Delta/\Omega_0 = -0.125$, and $\Gamma = 238$ (solid curve), $\Gamma = 0$ (dashed curve). The minimum values of $L(t)$ are 0.175 (solid curve) and 0.15 (dashed curve). (b) Probability density ($P = |\Psi(x,t)|^2$) of the atomic distribution at the time $t = t_m$ of the best atomic localization. The parameters are same as those of (a) with $t_m = 7 \times 10^{-3}$. The solid curve is almost indistinguishable from the dashed curve on the scale shown. For clarity, the close-up to the right of origin ($x = 0$) is shown in the inset.

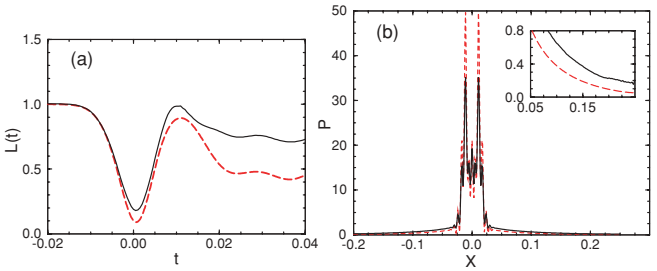

FIG. 11. (Color online) (a) Localization factor of the atomic distribution as a function of the dimensionless time t around its global minimum for the parameters $\sigma_t = 0.01$, $\Omega_0 = 4 \times 10^4$, $\Delta/\Omega_0 = -0.125$, and $\Gamma = 238$ (solid curve), $\Gamma = 0$ (dashed curve). The minimum values of $L(t)$ are 0.18 (solid curve) and 0.1 (dashed curve). (b) Probability density ($P = |\Psi(x,t)|^2$) of the atomic distribution at the time $t = t_m$ of the best atomic localization. The parameters are same as those of (a) with $t_m = 0$. For clarity, the close-up to the right of origin ($x = 0$) is shown in the inset.

add a recoil momentum to the atom [see Eqs. (18) and (22)]. After the collapse, the random number ε is renewed and the process gets repeated by solving again Eq. (23) starting from the new initial time $t_i = t_{MC}$ and the new values for the initial Fourier coefficients. This procedure gets continued until the final time t at which the calculation of the deposited atomic density should be performed. This results in a single quantum trajectory $\psi^s_{e,g}(x,t)$ obtained by normalizing the wave function Eq. (20) at the final time t. An ensemble average of many such trajectories [Eq. (17)] is statistically equivalent to the solution of the density matrix equations.

When the detuning of the light frequency is relatively large ($|\Delta| \gg \Omega_0$), the atoms primarily evolve in their ground state during the interaction with the light. In this case, the degradation of the atom focusing due to spontaneous emission is negligible as reported in earlier studies [6,16]. However, if a near-resonant light is used to focus the atomic beam, the spontaneous emission may broaden significantly the atomic distribution because of the random atomic recoils and fluctuations of the focusing potentials discussed above. These effects are particularly considerable in the case of atom focusing by red-detuned light fields, because the focusing then occurs near the light intensity maxima, resulting in substantial population of excited atoms. In order to measure this quantitatively, we again use the localization factor Eq. (15) with the atomic density $|\Psi(x,t)|^2$ given by Eq. (17). We find that an average of $N = 5000$ quantum trajectories is sufficient to give a statistical error below 2% of the mean value in Eq. (17). The results are shown with ($\Gamma = 238$) and without ($\Gamma = 0$) spontaneous decay of the atoms for the thin-lens (Fig. 10) and thick-lens (Fig. 11) focusing regimes. It is seen from the graphs that spontaneous emission does not shift the optimal time $t = t_m$ for the global minimum of the localization factor, but it reduces the atomic density and increases the background significantly in the thick-lens focusing of atoms.

V. SUMMARY

In this article we studied the spatial focusing of an atomic beam by a near-resonant SW light in the context of atom lithography. The problem was treated both classically and quantum-mechanically using the optimization approach suggested in Ref. [16] for the efficient focusing of atomic beams. We found that in the case of red detuning, the spherical aberrations of the periodic potential are reduced as the SW frequency gets closer to the atomic transition resonance, resulting in better focusing both in the thin- and thick-lens regimes. When the light mask is blue detuned, classical calculations show that near-resonance light degrades the localization. However, in the thin-lens regime, quantum-mechanical effects give rise to a new focusing mechanism that enhances the localization in this case. Finally, we considered the role of nonadiabatic transitions between the dressed atomic states and the effects of spontaneous emission of atoms on the quality of the deposition profile.

ACKNOWLEDGMENTS

We acknowledge fruitful discussions with D. Meschede, K. Mølmer, and T. Pfau. This work was supported by the German-Israeli Foundation (GIF) for Scientific Research and Development. This research is made possible in part by the historic generosity of the Harold Perlman Family.

[1] M. K. Oberthaler and T. Pfau, J. Phys. Condens. Matter **15**, R233 (2003).

[2] D. Meschede and H. Metcalf, J. Phys. D: Appl. Phys. **36**, R17 (2003).

[3] T. Sleator, T. Pfau, V. Balykin, and J. Mlynek, Appl. Phys. B: Photophys. Laser Chem. **54**, 375 (1992); G. Timp, R. E. Behringer, D. M. Tennant, J. E. Cunningham, M. Prentiss, and K. K. Berggren, Phys. Rev. Lett. **69**, 1636 (1992).

[4] K. K. Berggren, M. Prentiss, G. L. Timp, and R. E. Behringer, J. Opt. Soc. Am. B **11**, 1166 (1994).
[5] J. J. McClelland, J. Opt. Soc. Am. B **12**, 1761 (1995).
[6] J. L. Cohen, B. Dubetsky, and P. R. Berman, Phys. Rev. A **60**, 4886 (1999).
[7] M. K. Olsen, T. Wong, S. M. Tan, and D. F. Walls, Phys. Rev. A **53**, 3358 (1996).
[8] C. J. Lee, Phys. Rev. A **61**, 063604 (2000).
[9] V. Natarajan, R. E. Behringer, and G. Timp, Phys. Rev. A **53**, 4381 (1996); R. E. Behringer, V. Natarajan, and G. Timp, Opt. Lett. **22**, 114 (1997).
[10] J. J. McClelland, R. E. Scholten, E. C. Palm, and R. J. Celotta, Science **262**, 877 (1993); W. R. Anderson, C. C. Bradley, J. J. McClelland, and R. J. Celotta, Phys. Rev. A **59**, 2476 (1999).
[11] U. Drodofsky, J. Stuhler, B. Brezger, T. Schulze, M. Drewsen, T. Pfau, and J. Mlynek, Microelectron. Eng. **35**, 285 (1997); Th. Schulze, B. Brezger, P. O. Schmidt, R. Mertens, A. S. Bell, T. Pfau, and J. Mlynek, *ibid.* **46**, 105 (1999); Th. Schulze, T. Müther, D. Jürgens, B. Brezger, M. K. Oberthaler, T. Pfau, and J. Mlynek, Appl. Phys. Lett. **78**, 1781 (2001).
[12] R. W. McGowan, D. M. Giltner, and S. A. Lee, Opt. Lett. **20**, 2535 (1995).
[13] R. Ohmukai, S. Urabe, and M. Watanabe, Appl. Phys. B: Lasers Opt. **77**, 415 (2003).
[14] E. te Sligte, B. Smeets, K. M. R. van der Stam, R. W. Herfst, P. van der Straten, H. C. W. Beijerinck, and K. A. H. van Leeuwen, Appl. Phys. Lett. **85**, 4493 (2004); G. Myszkiewicz, J. Hohlfeld, A. J. Toonen, A. F. Van Etteger, O. I. Shklyarevskii, W. L. Meerts, Th. Rasing, and E. Jurdik, *ibid.* **85**, 3842 (2004).
[15] R. Gupta, J. J. McClelland, Z. J. Jabour, and R. J. Celotta, Appl. Phys. Lett. **67**, 1378 (1995); U. Drodofsky, J. Stuhler, T. Schulze, M. Drewsen, B. Brezger, T. Pfau, and J. Mlynek, Appl. Phys. B: Lasers Opt. **65**, 755 (1997).
[16] R. Arun, I. Sh. Averbukh, and T. Pfau, Phys. Rev. A **72**, 023417 (2005); M. Leibscher and I. Sh. Averbukh, *ibid.* **65**, 053816 (2002).
[17] D. Jürgens, A. Greiner, R. Stützle, E. te Sligte, A. Habenicht, and M. K. Oberthaler, Phys. Rev. Lett. **93**, 237402 (2004).
[18] I. Grigorenko, J. Chem. Phys. **128**, 104109 (2008).
[19] C. Cohen-Tannoudji, J. Dupont-Roc, and G. Grynberg, *Atom-Photon Interactions: Basic Processes and Applications* (Wiley, New York, 1998).
[20] More precisely, the condition for adiabatic following is $|\langle E_j(t)|\dot{H}(t)|E_i(t)\rangle| \ll |E_j(t)| - E_i(t)^2|$, where $|E_{i,j}(t)\rangle$ are the time-dependent dressed states (with eigenenergies $E_{i,j}(t)$) of the Hamiltonian $H(t)$. However, an approximate and simplified expression can be obtained by evaluating it using the bare atomic states and energies.
[21] In all figures, the probability density of the atomic distribution is normalized such that its integral over a standing wave period $(\lambda/2)$ is unity.
[22] D. Jürgens, Ph.D. dissertation, Universität Konstanz, Germany (2004).
[23] Note that the atom evolves primarily in its ground internal state outside the light region if the atom adiabatically follows the potential (4).
[24] This feature is present even if the light intensity profile is replaced by a steplike function: $\Omega(t) = \Omega_0$ for $|t| < \sigma_t$ and $\Omega(t) = 0$ for $|t| > \sigma_t$. However, we have found that the presence of chromatic aberrations and transverse velocity spread in the atomic beam would cancel this quantum localization of atoms in the thin-lens regime.
[25] K. Molmer, Y. Castin, and J. Dalibard, J. Opt. Soc. Am. B **10**, 524 (1993); R. Blatt, W. Ertmer, P. Zoller, and J. L. Hall, Phys. Rev. A **34**, 3022 (1986); R. Dum, P. Zoller, and H. Ritsch, *ibid.* **45**, 4879 (1992).
[26] M. D. Hoogerland, H. F. P. deBie, H. C. W. Beijerinck, E. J. D. Vredenbregt, K. A. H. van Leeuwen, P. vander Straten, and H. J. Metcalf, Phys. Rev. A **54**, 3206 (1996).